

# Effects of Partial Confinement on the Specificity of Monomolecular Alkane Reactions for Acid Sites in Side Pockets of Mordenite\*\*

Rajamani Gounder and Enrique Iglesia\*

The location of Brønsted acid sites within zeolites influences catalytic rates and selectivities when their diverse intra-channel environments stabilize transition states to different extents.<sup>[1]</sup> Mordenite zeolites in the proton form (H-MOR) contain acid sites located within two general environments: eight-membered ring (8-MR) side pockets and 12-MR main channels. The location of these acid sites can be determined by rigorous deconvolution of OH infrared bands and by titration with molecules of varying size,<sup>[2,3]</sup> allowing catalytic turnover rates to be described in terms of the respective contributions from sites within these two locations.

We have shown previously that monomolecular cracking and dehydrogenation of propane and *n*-butane occur preferentially within constrained 8-MR pockets, where transition states and adsorbed reactants are only partially confined.<sup>[2]</sup> Such configurations lead to entropy gains that compensate for the weaker binding of partially confined structures to give lower free energies for transition states within 8-MR pockets.<sup>[2]</sup> For *n*-alkanes, monomolecular dehydrogenation reactions show greater specificity for 8-MR locations than cracking and also show higher activation barriers,<sup>[2]</sup> predominantly because (C-H-H)<sup>+</sup> species involved in transition states for dehydrogenation reactions are less stable than the (C-C-H)<sup>+</sup> carbonium ions in cracking transition states (proponium,<sup>[4]</sup> *n*-butonium<sup>[5]</sup>). Activation entropies were also higher for *n*-alkane dehydrogenation than for cracking,<sup>[2]</sup> consistent with crossing potential curve descriptions of charge transfer reaction coordinates using,<sup>[6-8]</sup> which indicate that transition states with higher energies are looser and occur later along the reaction coordinates. Thus, it seems plausible that reactions involving later and looser transition states, with more fully formed ion pairs, benefit preferentially from entropy gains caused by partial confinement within 8-MR side pockets. The electrostatic underpinnings of these entropy benefits resemble those for proton-transfer<sup>[7]</sup> and electron-transfer<sup>[8]</sup> reactions in solvated systems, for which the entropies for molecular and charge reorganization are

essential in stabilizing the ion pairs formed upon charge transfer.

Here, we probe and extend these concepts of 8-MR pocket specificity in ion-pair stabilization to monomolecular reactions of branched alkanes. We show that isobutane cracking has a stronger preference for reaction within 8-MR locations in MOR than does dehydrogenation, in sharp contrast with the trends for *n*-alkane reactions. Transition state energies are higher for isobutane cracking than for dehydrogenation, consistent with the less stable cations formed upon protonation of C-C bonds instead of the tertiary C-H bond in isobutane.<sup>[9]</sup> We propose that, as for monomolecular *n*-alkane dehydrogenation, isobutane cracking shows a stronger preference for reaction on 8-MR acid sites than does dehydrogenation because it involves later and looser transition states, which benefit more strongly from entropy gains arising from partial confinement.

The fraction of the Brønsted acid sites located within 8-MR pockets varies widely (10–80%) among H-MOR samples<sup>[10]</sup> prepared by partial exchange of H<sup>+</sup> with Na<sup>+</sup> and also among H-MOR samples of different provenance.<sup>[2]</sup> Rate constants for monomolecular isobutane cracking (per total H<sup>+</sup>; 748 K; Figure 1a) and dehydrogenation (Figure 1b) increased monotonically as the fraction of the protons located within 8-MR pockets increased. As for *n*-alkanes, these data show that both reactions occur preferentially on sites located within 8-MR pockets. Isobutane cracking-to-dehydrogenation rate ratios *increased* with increasing 8-MR H<sup>+</sup> fraction, in contrast with those measured for propane and *n*-butane (Figure 2); thus, cracking shows a stronger kinetic preference for 8-MR sites than dehydrogenation for isobutane reactants (700–780 K; Section S.1, Supporting Information). The rate constants for isobutane dehydrogenation and cracking on 8-MR and 12-MR acid sites were extracted from their respective dependences on the number of sites at each location for each temperature (Section S.2, Supporting Information).<sup>[2]</sup> At 748 K, dehydrogenation rate constants were approximately 7 times larger on 8-MR than on 12-MR sites, while cracking rate constants were not detectable on 12-MR sites (Table 1).

Monomolecular alkane activation involves carbonium ion-like transition states<sup>[11,12]</sup> formed by interactions of adsorbed reactants (A<sub>z</sub>) with Brønsted acid sites (H<sup>+</sup>); adsorbed reactants are in quasi-equilibrium with those in the extracrystalline gas phase (A<sub>g</sub>; Scheme 1). Reaction rates [Eq. (1)] are first-order in alkane pressure (P<sub>A</sub>), where *k*<sub>int</sub> and

$$r = k_{\text{int}} K_A P_A = k_{\text{meas}} P_A \quad (1)$$

*k*<sub>meas</sub> are intrinsic and measured rate constants, respectively,

[\*] R. Gounder, Prof. E. Iglesia  
Department of Chemical Engineering  
University of California at Berkeley  
Berkeley, CA 94720 (USA)  
Fax: (+1) 510-642-4778  
E-mail: iglesias@cchem.berkeley.edu  
Homepage: <http://iglesia.cchem.berkeley.edu/>

[\*\*] We acknowledge with thanks the financial support from the Chevron Energy Technology Company. We also thank Dr. Stacey I. Zones (Chevron) and Prof. Matthew Neurock (University of Virginia) for valuable technical discussions.

Supporting information for this article is available on the WWW under <http://dx.doi.org/10.1002/anie.200905869>.

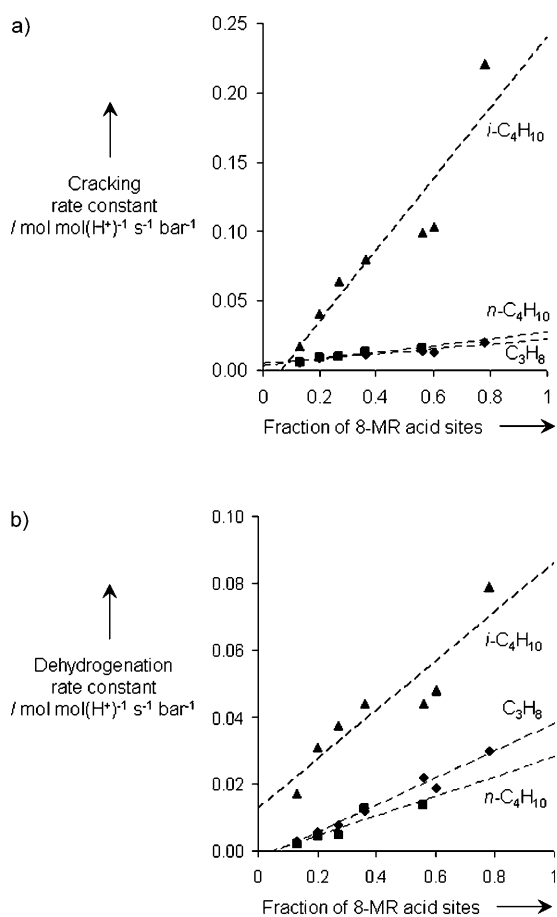


**Figure 1.** Dependence of rate constants (748 K) for monomolecular a) cracking and b) dehydrogenation of propane ( $\times 10$ ;  $\blacklozenge$ ), *n*-butane ( $\blacksquare$ ), and isobutane ( $\blacktriangle$ ) on the fraction of 8-MR acid sites in H-MOR catalysts.

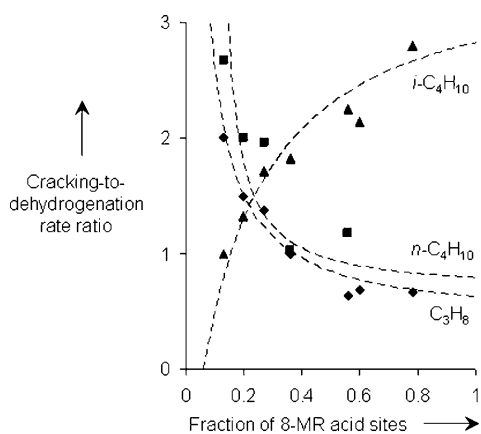


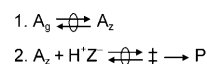
**Figure 2.** Cracking-to-dehydrogenation rate ratios (748 K) for propane ( $\blacklozenge$ ), *n*-butane ( $\blacksquare$ ) and isobutane ( $\blacktriangle$ ) on H-MOR catalysts with different fractions of Brønsted acid sites within 8-MR side pockets; rate ratios predicted using regressed rate constants are given by the dashed curves.

and  $K_A$  is the adsorption equilibrium constant (Section S.3, Supporting Information).<sup>[2,13–16]</sup> The combined temperature dependences of  $k_{\text{int}}$  and  $K_A$  show that  $k_{\text{meas}}$  depends only on

**Table 1:** Monomolecular isobutane cracking and dehydrogenation rate constants ( $k_{\text{meas}}$ ) at 748 K on acid sites within 8-MR and 12-MR locations of MOR.

Reaction	$k_{\text{meas}}$ (8-MR) <sup>[a]</sup>	$k_{\text{meas}}$ (12-MR) <sup>[a]</sup>
Cracking	$25.8 \pm 3.2$	n.d. <sup>[b]</sup>
Dehydrogenation	$9.1 \pm 1.0$	$1.3 \pm 0.7$

[a] [ $10^{-2} \text{ mol}(\text{mol H}^+)^{-1} \text{ s}^{-1} \text{ bar}^{-1}$ ]; rate parameters determined by linear regression methods; uncertainties reported as one standard deviation (details in Section S.2 of the Supporting Information). [b] n.d., not detected.



**Scheme 1.** Reaction sequence for monomolecular activation of alkanes (A) on Brønsted acid sites located within zeolite channels ( $\text{H}^+\text{Z}^-$ ) to form products (P); adapted from Ref. [2].

free-energy differences between gaseous reactants and transition states [Eq. (2)] and is determined solely by the consequences of confinement for transition state stability.

$$k_{\text{meas}} = \exp\left(-\left(\Delta G_{\ddagger}^{\circ} - \Delta G_{A_0}^{\circ}\right)/RT\right) \quad (2)$$

Cracking (C) to dehydrogenation (D) rate ratios reflect, in turn, differences in the stability of the ion pairs involved in their respective transition states [Eq. (3)]. This treatment

$$k_{\text{meas,C}}/k_{\text{meas,D}} = \exp\left(-\left(\Delta G_{\ddagger,\text{C}}^{\circ} - \Delta G_{\ddagger,\text{D}}^{\circ}\right)/RT\right) \quad (3)$$

highlights the pre-eminence of activation free energies, instead of the separate effects of activation entropies and enthalpies, in the dynamics of chemical reactions, a conclusion also evident from enthalpy–entropy compromises mediated by solvation within zeolite voids.

Measured activation barriers are 14–19  $\text{kJ mol}^{-1}$  larger for cracking than for dehydrogenation of isobutane on all MOR samples (Table 2), consistent with previous data on H-MFI

**Table 2:** Measured activation energies ( $E_{\text{meas}}$ ) for monomolecular isobutane cracking (C) and dehydrogenation (D) on MOR samples.

Zeolite	$E_{\text{meas,C}}^{\text{[a]}}$ [kJ mol <sup>-1</sup> ]	$E_{\text{meas,D}}^{\text{[b]}}$ [kJ mol <sup>-1</sup> ]
H <sub>100</sub> Na <sub>0</sub> MOR-T	191	177
H <sub>100</sub> Na <sub>0</sub> MOR-Z	208	194
H <sub>45</sub> Na <sub>55</sub> MOR-Z	205	186

[a]  $\pm 8 \text{ kJ mol}^{-1}$ . [b]  $\pm 15 \text{ kJ mol}^{-1}$ .

and H-USY<sup>[17–21]</sup> and with theoretical estimates on 20 T-atom MFI clusters.<sup>[22]</sup> Isobutane cracking-to-dehydrogenation rate ratios, as a result, increased with temperature (Figure 3), in sharp contrast with ratios that decreased with temperature for propane and *n*-butane, as a result of the larger barriers for *n*-alkane dehydrogenation than cracking.<sup>[2]</sup> We note that alkane cracking-to-dehydrogenation rate ratios that increased with temperature (Figure 3) also increased with the fraction of

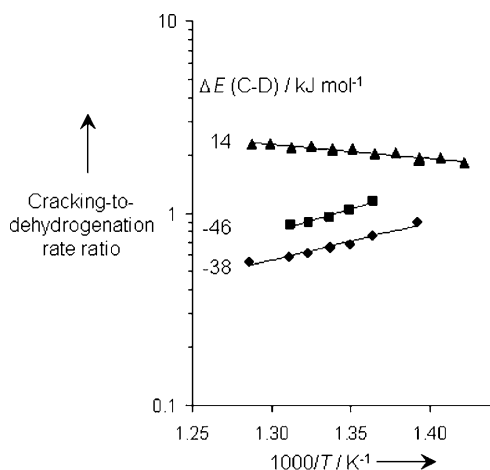


**Figure 3.** Dependence of monomolecular propane (◆), *n*-butane (■), and isobutane (▲) cracking-to-dehydrogenation rate ratios ( $H_{100}Na_0MOR-Z$ ) on temperature; differences in cracking (C) and dehydrogenation (D) activation energies are reflected in the slope.

protons within 8-MR pockets (Figure 2). We conclude that reaction paths with higher activation barriers show greater specificity for 8-MR locations, apparently because later and looser transition states involved in these paths capture a greater benefit from the entropy gains resulting from partial confinement.

Monomolecular cracking and dehydrogenation paths for normal alkanes<sup>[23,24]</sup> and isoalkanes<sup>[22,25,26]</sup> involve ion pairs with alkyl fragments containing a nearly full positive charge (+0.9). These transition states are stabilized by electrostatic interactions with the negatively charged framework and by van der Waals interactions that also stabilize adsorbed alkane reactants to the same extent. Born–Haber thermochemical cycles<sup>[2]</sup> (Section S.4, Supporting Information) indicate that differences in cracking and dehydrogenation barriers reflect predominantly enthalpy differences for protonation of C–C bonds and C–H bonds in gas-phase alkanes (Figure 4); this

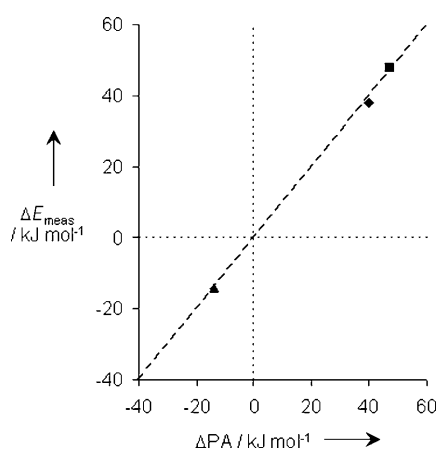


**Figure 4.** Difference in dehydrogenation and cracking activation barriers ( $\Delta E_{\text{meas}}$ ) measured on  $H_{100}Na_0MOR-Z$  for propane (◆), *n*-butane (■), and isobutane (▲) plotted against the difference in gas-phase proton affinities of their C–H and C–C bonds ( $\Delta PA$ ) (Section S.5, Supporting Information).

analysis also showed<sup>[2]</sup> that larger *n*-alkane dehydrogenation barriers reflect less stable cations formed upon protonation of C–H bonds instead of C–C bonds in *n*-alkanes.<sup>[4,5]</sup> Higher activation barriers for cracking than dehydrogenation of isobutane (by 14–19  $\text{kJ mol}^{-1}$ ; Table 2) reflect the less exothermic gas-phase protonation of C–C bonds ( $-682 \text{ kJ mol}^{-1}$ ) than of tertiary C–H bonds ( $-696 \text{ kJ mol}^{-1}$ ).<sup>[9]</sup> The resulting gas-phase cations are  $(\text{CH}_3)(i\text{-C}_3\text{H}_7^+)$  and  $(\text{H}_2)(\text{tert-C}_4\text{H}_9^+)$  van der Waals complexes formed by protonation of isobutane at its C–C and tertiary C–H bonds, respectively;<sup>[9]</sup> these structures resemble the fully formed ion pairs at late transition states for both reactions suggested by density functional theory.<sup>[22,25,26]</sup> Thus, we conclude that differences in monomolecular cracking and dehydrogenation barriers for linear and branched alkanes reflect enthalpy differences for gas-phase protonation at their C–C and C–H bonds (Figure 4), resulting in predictable effects of temperature (Figure 3) and acid site location (Figure 2) on selectivity.

Rate constants as a function of temperature can be used to estimate activation energies for cracking and dehydrogenation at 8-MR and 12-MR locations. Activation energies for monomolecular *n*-alkane cracking were higher on 8-MR than on 12-MR sites, because of weaker binding and less intimate van der Waals contacts for both reactants and transition states, which can be confined only partially within 8-MR pockets.<sup>[2]</sup> Activation energies for isobutane cracking and dehydrogenation on 8-MR acid sites were  $(188 \pm 8) \text{ kJ mol}^{-1}$  and  $(175 \pm 15) \text{ kJ mol}^{-1}$ , respectively. The rate constants on 12-MR sites were too small for accurate estimates of their activation energies. Thus, we infer that partial confinement of reactants and transition states within 8-MR pockets enables entropy–enthalpy compromises, as in the case of *n*-alkanes and consistent with geometric considerations.<sup>[27]</sup>

As for *n*-alkanes, we conclude that acid sites confined within 8-MR pockets are much more active for monomolecular isobutane reactions than sites of similar acid strength<sup>[28]</sup> within 12-MR channels (Table 3) because partially confined

**Table 3:** Ratio of 8-MR to 12-MR rate constants ( $k_{\text{meas}}$ ) at 748 K for monomolecular cracking and dehydrogenation of propane, *n*-butane and isobutane.

Reaction	$k_{\text{meas}}(8\text{-MR})/k_{\text{meas}}(12\text{-MR})$		
	Propane	<i>n</i> -Butane	Isobutane
Cracking	2.9	> 6.2 <sup>[a,b]</sup>	> 14.3 <sup>[b]</sup>
Dehydrogenation	> 10.7 <sup>[b]</sup>	> 15.8 <sup>[b]</sup>	6.8

[a] Total cracking rate ratio. Ratios are > 10.4 and 2.3 for terminal and central C–C cracking, respectively. [b] Rate constants on 12-MR sites were zero, within the error of regression. Lower limits on 8-MR-to-12-MR rate ratios were calculated from the maximum value of the 12-MR rate constant, estimated as the upper bound of the confidence interval containing one standard deviation.

transition states have lower standard free energies as a result of entropy–enthalpy trade-offs. These compromises and their dependence on catalyst structure appear to be ubiquitous and consequential for reactivity in acid catalysis as the concerted alignment of van der Waals contacts becomes ultimately unfavorable as a result of concomitant losses in rotational and

vibrational entropy in the transition state ion pairs. Entropy gains mediated by partial confinement benefit most strongly the highest energy transition states among possible parallel pathways, because they are looser and occur later along the reaction coordinate. Thus, for monomolecular alkane activation, the higher energy pathway involves the less stable protonated-alkane ion pair (Figure 4) and has a greater specificity for 8-MR locations in H-MOR (Figure 2).

These findings and concepts highlight the preeminent role of entropy and free energy in determining reactivity and selectivity in chemical reactions,<sup>[2,29,30]</sup> the strong effects of location in the preferential stabilization of specific transition states,<sup>[1,2]</sup> and the rigor of thermochemical analyses in dissecting the effects of catalyst and reactant properties on the stability of bound reactants and ion pairs at the transition state.

### Experimental Section

H-zeolites were prepared by treating  $\text{NH}_4^+$ -zeolites in flowing dry air ( $2.5 \text{ cm}^3 \text{ g}^{-1} \text{ s}^{-1}$ , zero grade, Praxair) at 773 K (at  $0.0167 \text{ K s}^{-1}$ ) for 4 h and then pelleting, crushing, and sieving to retain 180–250  $\mu\text{m}$  (60–80 mesh) aggregates. The methods used to prepare the  $\text{Na}^+$ -exchanged zeolites, determine their elemental composition and obtain  $^{27}\text{Al}$ -NMR and infrared spectra are reported elsewhere.<sup>[2]</sup> Catalytic cracking and dehydrogenation rates were measured under differential conditions (< 2% conversion) in a plug-flow tubular quartz reactor.<sup>[2]</sup> Catalysts (0.01–0.03 g) were first treated in a 5%  $\text{O}_2$ /95% He mixture ( $16.7 \text{ cm}^3 \text{ g}^{-1} \text{ s}^{-1}$ , 99.999%, Praxair) at 803 K ( $0.0167 \text{ K s}^{-1}$ ) for 2 h and then in pure He flow ( $16.7 \text{ cm}^3 \text{ g}^{-1} \text{ s}^{-1}$ , 99.999%, Praxair) for 0.5 h, while isobutane reactants (10%  $i\text{-C}_4\text{H}_{10}$ , 5% Ar, 85% He, Praxair, 99.5% purity) were transferred via heated lines (423 K) to a gas chromatograph (Agilent HP-6890GC) for calibration purposes. Flame ionization and thermal conductivity detection were used to measure reactants and products, which were separated chromatographically using GS-AL/KCl capillary (0.530 mm ID  $\times$  50 m; Agilent) and HayeSep DB packed (100–120 mesh, 10 ft.; Sigma–Aldrich) columns. Reactants were mixed with He (99.999%, Praxair) to vary  $i\text{-C}_4\text{H}_{10}$  pressures (1–5 kPa) and molar rates ( $10^{-4}$ – $10^{-3} \text{ mol alkane g}^{-1} \text{ s}^{-1}$ ). Equimolar  $\text{C}_3/\text{C}_1$  product ratios were observed at all space velocities; taken together with the absence of  $\text{C}_{5+}$  products, these data confirm that bimolecular or secondary pathways do not contribute to the products formed. Activation energies and pre-exponential factors were determined from rate constants measured as a function of temperature (703–778 K). Rates and selectivities measured after ca. 10 h on stream were similar (within 5%) to their initial values on all catalysts, indicating that deactivation did not influence kinetic data.

Received: October 19, 2009

Published online: December 16, 2009

**Keywords:** alkanes · cracking · dehydrogenation · mordenite · zeolites

- [1] A. Bhan, E. Iglesia, *Acc. Chem. Res.* **2008**, *41*, 559.
- [2] R. Gounder, E. Iglesia, *J. Am. Chem. Soc.* **2009**, *131*, 1958.
- [3] A. Bhan, A. D. Allian, G. J. Sunley, D. J. Law, E. Iglesia, *J. Am. Chem. Soc.* **2007**, *129*, 4919.
- [4] P. M. Esteves, C. J. A. Mota, A. Ramírez-Solís, R. Hernández-Lamonedá, *J. Am. Chem. Soc.* **1998**, *120*, 3213.
- [5] P. M. Esteves, G. G. P. Alberto, A. Ramírez-Solís, C. J. A. Mota, *J. Phys. Chem. A* **2000**, *104*, 6233.
- [6] J. Horiuti, M. Polanyi, *Acta Physicochim.* **1935**, *2*, 505.
- [7] R. P. Bell, *The Proton in Chemistry*, Chapman and Hall, London, **1973**.
- [8] R. A. Marcus, *Annu. Rev. Phys. Chem.* **1964**, *15*, 155.
- [9] C. J. A. Mota, P. M. Esteves, A. Ramírez-Solís, R. Hernández-Lamonedá, *J. Am. Chem. Soc.* **1997**, *119*, 5193.
- [10] Samples are labeled according to their fractional  $\text{H}^+$  and  $\text{Na}^+$  content and appended with a letter denoting their origin: Zeolyst (-Z), Süd-Chemie (-S), Tosoh (-T).
- [11] W. O. Haag, R. M. Dessau, *Proceedings—International Congress on Catalysis, 8th, Vol. 2*, Verlag Chemie, Weinheim, **1984**, p. 305.
- [12] S. Kotrel, H. Knözinger, B. C. Gates, *Microporous Mesoporous Mater.* **2000**, *35–36*, 11.
- [13] T. F. Narbeshuber, H. Vinek, J. A. Lercher, *J. Catal.* **1995**, *157*, 388.
- [14] W. O. Haag, *Stud. Surf. Sci. Catal.* **1994**, *84*, 1375.
- [15] J. A. van Bokhoven, B. A. Williams, W. Ji, D. C. Koningsberger, H. H. Kung, J. T. Miller, *J. Catal.* **2004**, *224*, 50.
- [16] S. M. Babitz, B. A. Williams, J. T. Miller, R. Q. Snurr, W. O. Haag, H. Kung, *Appl. Catal. A* **1999**, *179*, 71.
- [17] E. A. Lombardo, W. K. Hall, *J. Catal.* **1998**, *112*, 565.
- [18] C. Stefanadis, B. C. Gates, W. O. Haag, *J. Mol. Catal.* **1991**, *67*, 363.
- [19] T. F. Narbeshuber, A. Brait, K. Seshan, J. A. Lercher, *J. Catal.* **1997**, *172*, 127.
- [20] A. Corma, P. J. Miguel, A. V. Orchilles, *J. Catal.* **1994**, *145*, 171.
- [21] G. Yaluri, J. E. Rekoske, L. M. Aparicio, R. J. Madon, J. A. Dumesic, *J. Catal.* **1995**, *153*, 54.
- [22] I. Milas, M. A. C. Nascimento, *Chem. Phys. Lett.* **2003**, *373*, 379.
- [23] S. A. Zygmunt, L. A. Curtiss, P. Zapol, L. E. Iton, *J. Phys. Chem. B* **2000**, *104*, 1944.
- [24] M. V. Frash, R. A. van Santen, *Top. Catal.* **1999**, *9*, 191.
- [25] V. B. Kazansky, M. V. Frash, R. A. van Santen, *Appl. Catal. A* **1996**, *146*, 225.
- [26] X. Zheng, P. Blowers, *J. Phys. Chem. A* **2006**, *110*, 2455.
- [27] a) The kinetic diameter of isobutane is 0.50 nm and of a methyl group is 0.38 nm (D. W. Breck, *Zeolite Molecular Sieves*, Wiley, New York, **1974**, pp. 633–641); b) the 8-MR pocket diameter is 0.41 nm and depth is 0.37 nm (R. Gounder, E. Iglesia, *J. Am. Chem. Soc.* **2009**, *131*, 1958).
- [28] M. Brändle, J. Sauer, *J. Am. Chem. Soc.* **1998**, *120*, 1556.
- [29] A. Bhan, R. Gounder, J. Macht, E. Iglesia, *J. Catal.* **2008**, *253*, 221.
- [30] R. A. van Santen, M. Neurock, *Molecular Heterogeneous Catalysis*, Wiley-VCH, Weinheim, **2006**.